Reconstruction of Atomistic Models of Dislocations by Means of Finite Deformation Theory

Paweł DŁUŻEWSKI[1)*], Kinga NALEPKA[2)]

[1)] *Institute of Fundamental Technological Research, Polish Academy of Sciences, Pawińskiego 5B, 02-106 Warsaw, Poland*

[2)] *AGH University of Krakow, Faculty of Mechanical Engineering and Robotics, Department of Machine Design and Maintenance, Al. Mickiewicza 30, 30-059 Kraków, Poland*

[*] *Corresponding Author e-mail: pdluzew@ippt.pan.pl*

The present paper discusses mathematical barriers in the development of software for preprocessing of atomistic models of dislocation networks. As a matter of fact, as yet, there are neither analytical nor numerical methods nor programs available which can be used for atomistic reconstruction of complex dislocation networks. Some of the problems to overcome are discussed in this paper. In the previous papers discussed below it was shown that a direct superposition of analytic formulae for displacements of atoms induced by single dislocations does not give possibility to hold the essential geometric properties of the resultant atomistic models. Namely, after the input of first dislocation, the lattice symmetry required to input the next dislocations is usually broken. These inaccuracies compose the mathematical barrier for atomistic reconstruction of advanced dislocation nets. A method developed here has been applied to reconstruction of the dislocation nodes localized in the copper/shaffire interface. In the present case, the partial dislocations are inserted by slips. For comparison, the junction corresponding to the stacking faults obtained by the rigid shifts of copper on the Burgers vector $\frac{1}{6}\langle 112 \rangle$ are discussed.

Keywords: dislocations, lattice distortions, finite deformations, atomistic models.

1. Introduction

In the computer modelling of engineering structures, the preprocessing of input data often plays a very important role. For example, to solve any Finite Element problem the structure must be discretized first into the FE mesh. Such a mesh must comprise all important details concerning the geometry and material properties. If the structure is more advanced then the meshing

presents a more complex problem. As a result, the prices of good programs for preprocessing of input data in some cases exceed the prices of programs used to solve the main FE problem. How does the preprocessing of input data look like in the atomistic modelling of dislocations? In fact, so far, there are no analytical nor numerical programs available by the use of which a fixed dislocation network with arbitrary chosen angles between dislocation segments can be preprocessed. For example, in molecular dynamics a random dislocation net is obtained by plastic deformation.

Dislocations play a very important role in prediction of various physical and chemical properties of nanostructures. Despite the very promising electronic properties of many semiconductor devices, the formation of crystal defects during the growth compose a technological barrier for the use of such materials in the production of electronic devices [19]. Recently, the analytic solutions obtained by means of the linear theory of elasticity have been used in the preprocessing of input data for atomistic modelling of many physical and/or chemical properties of dislocations [3–5, 9, 12, 22, 25, 28, 31, 40, 42]. Various dislocations are analysed by means of the ab-initio and atomistic methods. To compare the properties of different dislocation networks, their atomistic models are indispensable. Unfortunately, by using two different interatomic potentials two mutually different misfit dislocation patterns are often obtained. For many structures, this is because there are no reliable interatomic potentials that can gather the complex character of chemical bonding in a relatively simple form. Such a situation concerns among others the Cu/α-Al_2O_3 heterostructure considered in this paper, cf. [10, 26, 30, 32]. Ab-initio calculations are considerably a much more accurate method and provide essential information on the arrangement of atoms and bonds occurring in structures with defects as well as in heterostructures such as metal/oxide interfaces. Unfortunately, ab-initio methods can be applied only to small systems of atoms. Therefore, parallel studies for larger systems are undertaken by means of the molecular dynamics, molecular statics (MD/MS), Monte Carlo and other methods. The results obtained by MD/MS often depend on the assumed initial configuration of atoms. Thus, the aim of this paper is to develop a computational method which allows the preprocessing of a given variant of an atomistic system of dislocations enabling mutual fitting of two phases. There arises a question: *Is it possible at all to prepare such atomistic models of dislocation network in a deterministic manner?* Over fifty years ago, a similar question was stated in the context of the possibility of obtaining analytic formulae for lattice distortions induced by dislocations. Thanks to papers by Burgers [7], Yoffe [38, 39] and others that problem has been solved, first for isotropic elastic continuum, and thereafter step-by-step the analytical problems were solved also for anisotropic materials. Recently, for an arbitrarily chosen dislocation network composed of a finite number of dislocation elements,

the respective stress/distortion tensor field can be obtained using analytical methods.

It is worth emphasizing that despite the richness of analytical solutions available for anisotropic elasticity, and despite that most crystals demonstrate an anisotropic behaviour, in practice the most popular analytical equations in use concern the isotropic continuum, cf. [2, 18, 21]. Usually, the reason for this situation is rationalized by a small difference between the stress/strain fields obtained for isotropic and anisotropic continua. No less important for this situation is the complex analytical form of the equations obtained for anisotropic materials.

In this paper, our attention is focused on preprocessing of atomistic models by means of computational methods. It concerns the interfacial regions containing dislocations and stacking faults. The next section briefly presents the mathematical foundations of the nonlinear continuum theory of dislocations. In the literature, a term *the nonlinear theory of dislocations* is understood differently, and different notations are used. Our approach refers back to the papers by Kröner [24] and Teodosiu [37] where the so-called local relaxed configuration is employed to refer all crystallographic parameters to the perfect lattice. The transition between the current and the local relaxed configurations is carried out locally for material points. Such an approach is based on the use of immobile coordinate systems, Lagrangian and Eulerian, that are related to the initial and the current configurations, respectively. An alternative formulation, which is not used here, is based on the idea of a coordinate system being convected together with the crystal lattice. Then, the components of lattice deformation gradient form a unit matrix, while the role of deformation measures is taken by the metric tensor and asymmetric connection coefficients, cf. [6, 23].

2. Continuum theory of discrete dislocations

In the linear theory of dislocations, the gradient of crystal deformation is decomposed additively into the lattice and plastic distortion tensors, according to

$$\operatorname{grad} \mathbf{u} = \boldsymbol{\beta} + \boldsymbol{\beta}_{\mathrm{pl}}, \tag{1}$$

cf. [24] and [15]. By assumption, the lattice distortion $\boldsymbol{\beta}$ is composed of the antisymmetric tensor of crystal lattice rotation and the symmetric tensor of elastic strain, respectively,

$$\boldsymbol{\beta} = \mathbf{w} + \boldsymbol{\varepsilon}. \tag{2}$$

The plastic distortion $\boldsymbol{\beta}_{\mathrm{pl}}$ is identified with an asymmetric strain tensor that being isoclinic with the lattice rotation. This nomenclature comes from the theory of elasto-plastic Cosserat continua where the particle rotation $\boldsymbol{\chi}$ and its elastic/

plastic strains are identified, respectively with: $\boldsymbol{\chi} \equiv \mathbf{w}$, $\boldsymbol{\epsilon} \equiv \boldsymbol{\varepsilon}$, and $\boldsymbol{\epsilon}_{\mathrm{pl}} \equiv \boldsymbol{\beta}_{\mathrm{pl}}$; which gives

$$\operatorname{grad} \mathbf{u} = \boldsymbol{\chi} + \boldsymbol{\epsilon} + \boldsymbol{\epsilon}_{\mathrm{pl}}. \tag{3}$$

Contrary to the Cosserat continua, in the classical continuum theories of dislocations it is assumed that the material particles cannot rotate independently of the displacement field. This leads to the symmetry of the elastic strain tensor, and therefore a simplified notation gathering together the elastic strain and crystal lattice rotation into a common lattice distortion tensor, $\boldsymbol{\beta}$, is more convenient. According to the notation used in this paper, the multiplicative decomposition of the (total) deformation gradient into the lattice and the plastic deformations can be rewritten in the following form

$$\mathbf{F}_{\mathrm{tot}} = \mathbf{F}\,\mathbf{F}_{\mathrm{pl}}. \tag{4}$$

For chemically homogeneous crystals, $\mathbf{F}$ is identical to the elastic deformation tensor. For heterostructures, the situation is more complex, cf. [14].

The integration of lattice distortions over Burgers circuits can be performed over the spatial (deformed) or reference (perfect lattice) configurations according to the formulae

$$\begin{aligned} \mathbf{b} &= \oint_{\mathrm{c}} d\mathbf{x} = \oint_{\mathrm{O}} \mathbf{F}\, d\mathbf{X} = \oint_{\mathrm{c}} (\mathbf{1} + \widehat{\boldsymbol{\beta}})\, d\mathbf{X} = \oint_{\mathrm{c}} \widehat{\boldsymbol{\beta}}\, d\mathbf{X}, \\ -\widehat{\mathbf{b}} &= \oint_{\mathrm{C}} d\mathbf{X} = \oint_{\mathrm{o}} \mathbf{F}^{-1} d\mathbf{x} = \oint_{\mathrm{o}} (\mathbf{1} - \boldsymbol{\beta})\, d\mathbf{x} = - \oint_{\mathrm{o}} \boldsymbol{\beta}\, d\mathbf{x}, \end{aligned} \tag{5}$$

where $\mathbf{1}$ is the metric tensor of the Euclidean space; $\mathbf{b}$ and $\widehat{\mathbf{b}}$ are the spatial and so-called true Burgers vectors, respectively; the symbols c, C and o, O mean the open and closed Burgers circuits situated in the spatial (Eulerian) and reference configurations, respectively. In our approach the reference configuration is a counterpart of the local relaxed isoclinic configuration introduced by Teodosiu [37]. It is worth emphasising that the lattice distortion tensor $\boldsymbol{\beta}$ is related to the lattice spacings in the current configuration. Alternatively, the distortions can be pulled back by differentiation over the lattice spacings in the perfect lattice, which gives the following, mathematically strict and mutually reversible, transformation rule

$$\widehat{\boldsymbol{\beta}} = (\mathbf{1} - \boldsymbol{\beta})^{-1} - \mathbf{1}. \tag{6}$$

In the linear theory, the difference between differentiation over the spatial and reference configurations are neglected, i.e. it is assumed that $\boldsymbol{\beta} = \frac{\partial \mathbf{u}}{\partial \mathbf{x}} \approx \frac{\partial \mathbf{u}}{\partial \mathbf{X}} = \widehat{\boldsymbol{\beta}}$,

$\mathbf{F} \approx \mathbf{F}^{-1} \approx \mathbf{1}$, $O \equiv o$, etc. For such a simplification, the differential equations reduce to the linear equation set and, through the analytical methods available, many very useful formulae can be derived. On the other hand, most of the analogical nonlinear problems have not yet been solved analytically for dislocations. According to the finite deformation theory developed for immobile coordinate systems the deformation and distortion tensors satisfy the following mathematically strict and mutually reversible relations

$$\mathbf{F} = \mathbf{1} + \widehat{\boldsymbol{\beta}}, \qquad \mathbf{F}^{-1} = \left(\mathbf{1} - \boldsymbol{\beta}\right)^{-1}. \tag{7}$$

Unusually, the relationship on the left hand is employed to the operation on tensors referred to the local relaxed configuration while the relationship on the right is applied to tensor fields performed on the spatial configuration.

3. Analytical equations for mixed dislocation

The displacement vector field forming a mixed straight-line dislocation in an isotropic elastic material was determined first by Love [27]. The vector equations were presented in a few different forms, cf. [13, 34]. For the needs of the present paper, the respective equations can be rewritten in the following form

$$\mathbf{u}(\mathbf{x}) = \mathbf{f}(\mathbf{x}) = \mathbf{f}^a(\mathbf{x}) + \mathbf{f}^b(\mathbf{x}), \tag{8}$$

where the sequential components of the vector fields added are:

$$
\begin{aligned}
f_1^a &= \frac{b_1}{2\pi}\left(\operatorname{atan2}\left(\frac{y}{x}\right)x_2 x_1 + \frac{x_1}{x_2}2(1-\nu)(x_1^2 + x_2^2)\right) \\
&\quad - b_1\, H\left(\operatorname{atan2}\left(\frac{y}{x}\right)x_2 x_1 - \varphi\right), \\
f_2^a &= -\frac{b_1}{2\pi}\left(\frac{1-2\nu}{4(1-\nu)}\ln\frac{x_1^2 + x_2^2}{r_\circ^2} + \frac{x_1^2 - x_2^2}{4(1-\nu)(x_1^2 + x_2^2)}\right), \\
f_3^a &= \frac{b_3}{2\pi}\operatorname{atan2}\left(\frac{y}{x}\right)x_2 x_1;
\end{aligned}
\tag{9}
$$

$$
\begin{aligned}
f_1^b &= -\widehat{b}_1\, H(-\varphi), \\
f_2^b &= 0, \\
f_3^b &= 0.
\end{aligned}
\tag{10}
$$

The variables $\widehat{b}_1$ and $\widehat{b}_3$ are the edge and screw components of the true Burgers vector. The symbols ν and φ denote the Poisson ratio and the angle between

the edge component and the crystal plane along which the partial dislocation is introduced into the perfect lattice. The radius $r_\circ$ is used here to normalize the vertical shift of atoms in dislocation core, cf. $(9)_2$ and Table 1 with (3-46) in [21]. The present formula allows one to introduce a perfect or partial dislocation by slip, climb or in the mixed path, cf. Fig. 1. The Heaviside step function and $\text{atan2}\left(\frac{y}{x}\right)$ are defined according to the following convention:

$$H(x) \overset{df}{=} \begin{cases} 1 & x \geq 0, \\ 0 & x < 0, \end{cases}$$

$$\text{atan2}\left(\frac{y}{x}\right) \overset{df}{=} \begin{cases} \arctan\dfrac{y}{x} & x > 0, \\[2mm] \arctan\dfrac{y}{x} + \pi & y \geq 0, \ x < 0, \\[2mm] \arctan\dfrac{y}{x} - \pi & y < 0, \ x < 0, \\[2mm] 0 & x = 0. \end{cases} \tag{11}$$

Those definitions differ significantly from that mainly used in mathematics. Namely, the most well known definitions are:

$$H(x) \overset{df}{=} \begin{cases} 1 & x > 0, \\[1mm] \dfrac{1}{2}, & x = 0, \\[2mm] 0 & x < 0, \end{cases}$$

$$\text{atan2}\left(\frac{y}{x}\right) \overset{df}{=} \begin{cases} \arctan\dfrac{y}{x} & x > 0, \\[2mm] \arctan\dfrac{y}{x} + \pi & y \geq 0, \ x < 0, \\[2mm] \arctan\dfrac{y}{x} - \pi & y < 0, \ x < 0, \\[2mm] +\dfrac{\pi}{2} & y \geq 0, \ x = 0, \\[2mm] -\dfrac{\pi}{2} & y < 0, \ x = 0. \end{cases} \tag{12}$$

It is also worth mentioning that the function $\text{atan2}\left(\frac{y}{x}\right)$ depends not only on the factor $\frac{y}{x}$ but also on the signs of x and y. Thus the bar separating x and y in $\text{atan2}\left(\frac{y}{x}\right)$ is an inherent part of the notation applied.
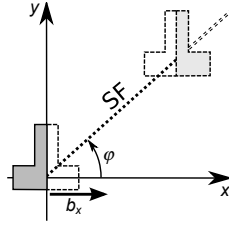
Fig. 1. Partial dislocation and stacking fault.

Table 1. Length scale effect on vertical displacement [Å] of points situated in vicinity of dislocation core.

Measure	Distance (X,Y) from dislocation core (in Å)		
	$\left(1, \frac{1}{100}\right)$	$\left(1, \frac{1}{10}\right)$	$(1, 1)$
[m]	3.19571	3.15737	2.89209
[n m]	0.76848	0.73015	0.46484
[Å]	0.49879	0.46045	0.19516
$r_\circ = b_1$	0.63462	0.59628	0.33099

Differentiation of (9) gives the following functions for lattice distortion:

$$\beta_{11} = \frac{-b_1}{2\pi} \frac{(3 - 2\nu)x_1^2 x_2 + (1 - 2\nu)x_2^3}{2(1 - \nu)(x_1^2 + x_2^2)^2},$$

$$\beta_{12} = \frac{b_1}{2\pi} \frac{(3 - 2\nu)x_1^3 + (1 - 2\nu)x_1 x_2^2}{2(1 - \nu)(x_1^2 + x_2^2)^2},$$

$$\beta_{21} = \frac{-b_1}{2\pi} \frac{(1 - 2\nu)x_1^3 + (3 - 2\nu)x_1 x_2^2}{2(1 - \nu)(x_1^2 + x_2^2)^2},$$

$$\beta_{22} = \frac{b_1}{2\pi} \frac{(1 + 2\nu)x_1^2 x_2 - (1 - 2\nu)x_2^3}{2(1 - \nu)(x_1^2 + x_2^2)^2},$$

$$\beta_{31} = \frac{-b_3}{2\pi} \frac{x_2}{x_1^2 + x_2^2},$$

$$\beta_{32} = \frac{b_3}{2\pi} \frac{x_1}{x_1^2 + x_2^2}.$$

$$(13)$$

The plastic distortion tensor field obtained by differentiation of the Heaviside and atan2 functions is not discussed here. It is worth noting only that for angle $\varphi = 0$ the non vanishing components are:

$$\beta_{\mathrm{pl}\,12} = -\widehat{b}_1\, \delta(y)\, H(-x),$$

$$\beta_{\mathrm{pl}\,32} = -\widehat{b}_3\, \delta(y)\, H(-x),$$

$$(14)$$

where δ denotes the Dirac function. More details on the decomposition of the total distortion gradient into the lattice curvature and dislocation tensor fields have been discussed recently in [15].

4. Atomistic reconstruction of dislocations

The linear theory of deformation, as a simplified theory, does not distinguish between the differentiation displacements over the reference and spatial configurations. One can check that in order to hold the symmetry of lattice distortion in the spatial (real) configuration, the distortion tensor field for atoms forming a given dislocation must be related to the spatial configuration. Unfortunately, the process of atomistic reconstruction of a dislocation cannot start from the spatial (wanted) configuration but from the reference one. In other words, with respect to the missing the current configuration, instead of pull back displacement field, $\mathbf{u} = \mathbf{f}(\mathbf{x})$, the mentioned analytic formulas are applied to push forward the atoms from a perfect lattice configuration. This corresponds to the following scheme

$$\mathbf{u} = \mathbf{f}(\mathbf{X}), \tag{15}$$

where $\mathbf{X} = \mathbf{x} - \mathbf{u}$, cf. (8), (9). This results in a broken symmetry of the lattice distortion field in such obtained spatial configuration of atoms. Obviously, the deviation from the correct positions, holding the symmetry of analytical fields applied is weekly visible in such reconstructed models of a single dislocation. The problem is that the errors usually accumulate with the sequential introduction of next dislocations into the atomistic model. To avoid these errors, another displacement function being consistent with analytical ones (8), (9) must be used. From the mathematical point of view, in order to introduce a dislocation directly from the perfect lattice, instead of (15), the wanted analytical function $\mathbf{u}(\mathbf{X})$ should satisfy the following formula

$$\mathbf{u} = \bar{\mathbf{f}}(\mathbf{X}) = \mathbf{f}(\mathbf{X} + \mathbf{u}). \tag{16}$$

The analytical solution of the implicit equation set (16) with respect to $\bar{\mathbf{f}}(*)$ obtained for a given $\mathbf{f}(*)$ is not a trivial analytical problem. For the present authors it is unknown whether the analytical form of $\bar{\mathbf{f}}(*)$ has ever been derived and how such a solution does look like. Anyway, Eq. (16) can be solved numerically by means of iterative methods. Let us consider the iteration of the displacement vector for the atom occupying the initial position $\mathbf{X}$. The displacement vector can be determined by using the iterative formula

$$\mathbf{u}^{i+1} = \mathbf{u}^i + \Delta\mathbf{u}^{i+1}. \tag{17}$$

In case of use of the Newton–Raphson method the correction is

$$\Delta\,\mathbf{u}^{i+1} = -\left(\frac{\Psi(\mathbf{X},\mathbf{u})}{\mathbf{u}}\right)^{-1}_{\mathbf{u}=\mathbf{u}^i}\Psi(\mathbf{u}^i), \tag{18}$$

where

$$\Psi(\mathbf{X},\mathbf{u}) \stackrel{df}{=} \mathbf{u} - \mathbf{f}(\mathbf{X}+\mathbf{u}). \tag{19}$$

Taking into account that locally $\boldsymbol{\beta} = \operatorname{grad}\mathbf{u}$, it is easy to prove that $\frac{\partial\Psi(\mathbf{X},\mathbf{u})}{\partial\mathbf{u}} = \frac{\partial\Psi(\mathbf{X},\mathbf{u})}{\partial\mathbf{x}}\frac{\partial\mathbf{x}}{\partial\mathbf{u}} = \mathbf{1} - \boldsymbol{\beta}(\mathbf{x})$, which gives the following resultant formula for iterating the position of a given atom in the spatial configuration

$$\Delta\,\mathbf{u}^{i+1} = -\left[\mathbf{1} - \boldsymbol{\beta}(\mathbf{X}+\mathbf{u}^i)\right]^{-1}\left[\mathbf{u}^i - \mathbf{f}(\mathbf{X}+\mathbf{u}^i)\right], \tag{20}$$

where $\mathbf{f}(\mathbf{x})$ and $\boldsymbol{\beta}(\mathbf{x})$ are identified with (8), (9), and (13) stated in the spatial configuration.

In our case the proposed nonlinear equation set, $\boldsymbol{\Psi}(\mathbf{u}) = \mathbf{0}$, was solved using a modified version of the Powell hybrid method [33]. In each iteration, the algorithm first determined the standard Newton step. If this step fell within the "trusted region" it was used as a trial step. Otherwise, linear combinations of the Newton and gradient directions were employed. In the previous papers the calculations have been performed for reconstruction of different positions of a perfect edge dislocation cores in hexagonal GaN and 4H-SiC crystals [12, 42].

Below we present another application of this approach to the reconstruction of atomistic models of misfit dislocation network between the copper layer and corundum substrate.

5. Reconstruction of dislocation networks

In the linear theory of dislocations the stress, strain and lattice distortion tensor fields corresponding to elemental dislocations are superposed in the spatial configuration. Such an obtained stress field holds the equilibrium equation, while the total distortion field satisfies the conditions stated for the true Burgers vectors. Namely, for two arbitrarily chosen dislocations differing each other from in their position and orientation, the integration of the total distortion field in the spatial configuration holds the following formulae:

$$\widehat{\mathbf{b}}_1 = \oint_{o_1}(\boldsymbol{\beta}_1 + \boldsymbol{\beta}_2)\,d\mathbf{x},$$

$$\widehat{\mathbf{b}}_1 + \widehat{\mathbf{b}}_2 = \oint_{o_{1+2}}(\boldsymbol{\beta}_1 + \boldsymbol{\beta}_2)\,d\mathbf{x}, \tag{21}$$

where o_1, o_{1+2} denote Burgers contours circled around the first and both dislocations in the spatial configuration, $\widehat{\mathbf{b}}_1$ and $\widehat{\mathbf{b}}_2$ are the true Burgers vectors which by definition satisfy $(5)_2$ for $\boldsymbol{\beta}_1(\mathbf{x})$ and $\boldsymbol{\beta}_2(\mathbf{x})$, respectively. Unfortunately, the summation of the respective displacement fields, $\mathbf{f}_1(\mathbf{x})$ and $\mathbf{f}_2(\mathbf{x})$, can result in formation of voids or overlapping atoms. In some cases such artifacts can be avoided, for example by glide of all dislocations on the same slip plane, if possible. Such an example is considered further.

Consider the reconstruction of a set of misfit dislocations formed between the copper layer and the corundum substrate [16, 17, 20, 29]. A mechanism of formation the misfit dislocations suggested by Dimitriev *et al.* [16, 17] is shown in Fig. 2. The authors considered the dissociation of initially perfect misfit dislocations into the partial ones and of formation of stacking-fault regions; see shaded triangles in Fig. 2. The corundum lattice can be terminated either by an aluminium (stoichiometric case) or an oxygen layer (oxygen rich interface) [35].
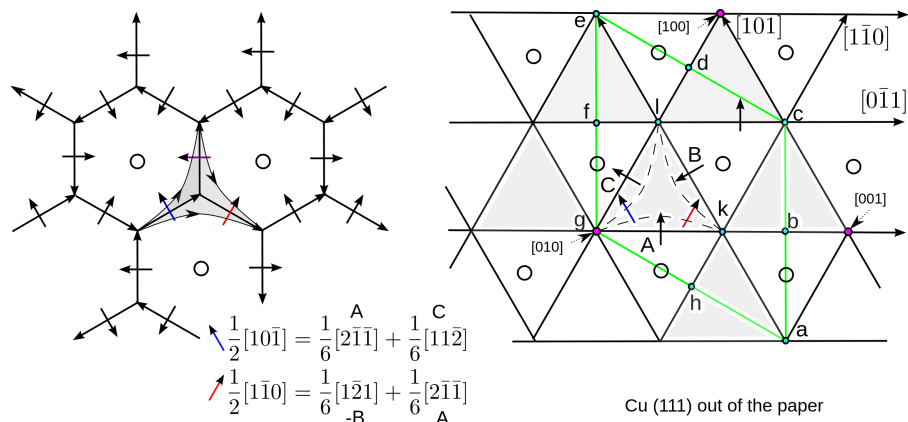

$$\frac{1}{2}[10\bar{1}] = \frac{1}{6}[2\bar{1}\bar{1}] + \frac{1}{6}[11\bar{2}]$$

$$\frac{1}{2}[1\bar{1}0] = \frac{1}{6}[1\bar{2}1] + \frac{1}{6}[2\bar{1}\bar{1}]$$

Cu (111) out of the paper

FIG. 2. Misfit dislocations in $\frac{\mathrm{Cu}[0\bar{1}1](111)}{\mathrm{Al_2O_3}[\bar{1}100](0001)}$ zone related to crystallographic directions in copper. Green parallelogram denotes the periodicity cell of the heterostructure with misfit dislocation network. Dashed lines on the right denote the transient position of partial dislocations taken in the dissociation process.

TABLE 2. Dislocations from Fig. 2 related to crystallographic directions in $\mathrm{Al_2O_3}$.

Dislocation number	Burgers vector	Line direction
A	$\frac{1}{9}[1\bar{2}10]$	$[\bar{1}010]$
B	$\frac{1}{9}[\bar{1}\bar{1}20]$	$[\bar{1}100]$
C	$\frac{1}{9}[2\bar{1}\bar{1}0]$	$[0\bar{1}10]$

In this example, in order to introduce misfit dislocations, the copper lattice has been stretched coherently to the corundum by coinciding the $[0\bar{1}1]$ direction in copper with $[\bar{1}100]$ in corundum. In such an assumed coherent junction, the outer copper atoms were situated on top of oxygen atoms at a distance of 1.827Å from the outer aluminum layer [36, 41]. A misfit dislocation recognized as a perfect one $\frac{1}{2}[0\bar{1}1]$ in copper, and is found to be a partial one in terms of the corundum unit cell. Nevertheless, the physical length of the Burgers vector is independent of the structure referred to, that is

$$\widehat{b} = \frac{\sqrt{2}}{2}\widetilde{a}_{\mathrm{Cu}} = \frac{\sqrt{3}}{3}\widehat{a}_{\mathrm{Al_2O_3}}, \tag{22}$$

where $\widetilde{a}$ denotes the size of the copper unit cell stretched to the relaxed corundum lattice, i.e., $\sqrt{3}\widetilde{a}_{\mathrm{Cu}} = \sqrt{2}\widehat{a}_{\mathrm{Al_2O_3}}$. Thus, the dissociation considered can be related to the copper or corundum unit cells, which gives:

$$\frac{1}{2}\langle 0\bar{1}1\rangle = \frac{1}{6}\langle \bar{1}\bar{1}2\rangle + \frac{1}{6}\langle 1\bar{2}1\rangle \tag{23}_1$$

as referred to copper,

$$\frac{1}{3}\langle \bar{1}100\rangle = \frac{1}{9}\langle \bar{1}2\bar{1}0\rangle + \frac{1}{9}\langle \bar{2}110\rangle \tag{23}_2$$

as referred to corundum.

Taking into account the parameters of the perfect lattices $\widehat{a}_{\mathrm{Cu}} = 3.615$Å, $\widehat{a}_{\mathrm{Al_2O_3}} = 4.7587$Å, the misfit related to the common reference configuration is

$$\frac{\frac{\sqrt{2}}{\sqrt{3}}\widehat{a}_{\mathrm{Al_2O_3}} - \widehat{a}_{\mathrm{Cu}}}{\widehat{a}_{\mathrm{Cu}}} = 0.0748167. \tag{24}$$

Thus, the distance between the perfect dislocations is $\frac{1}{0.0748167}a_{\mathrm{Al_2O_3}} \approx 14\,a_{\mathrm{Al_2O_3}}$. In our example, all partial dislocations were inserted simultaneously by the glide on the interfacial crystal plane intersecting the copper and corundum. Each family of mutually parallel partial dislocations is represented by a single dislocation piercing the chosen nodal point. Contrary to many atomistic methods which work only on periodic volume cells, this method does not impose, by default, the periodicity on resultant atomistic models. The method can work with an arbitrary chosen subregion of a perfect lattice to which the dislocations are inserted. In our example, a region with $2820 + 1880 + 2820$ atoms of Cu, Al and O was chosen for visualization and to check how the reconstructed regions look like in the sequential cells, respectively. In order to show what patterns of atomic bonds have been formed on the border of the stacking fault region and

coherent region, the considerably smaller numbers of atoms have been chosen for visualization in Figs. 3 and 4. The Love analytic solution for single dislocations applied here concerns a single straight-line dislocation in an infinite large elastic continuum. The superposition of all elemental tensor fields caused by elemental dislocations forms a total lattice distortion tensor field, which is used next to reconstruction of an atomistic model. Inserting a periodic bundle of mutually parallel misfit dislocations into perfect lattice (space), a semi-periodic volume
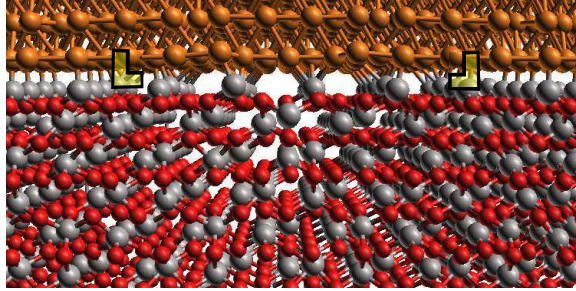

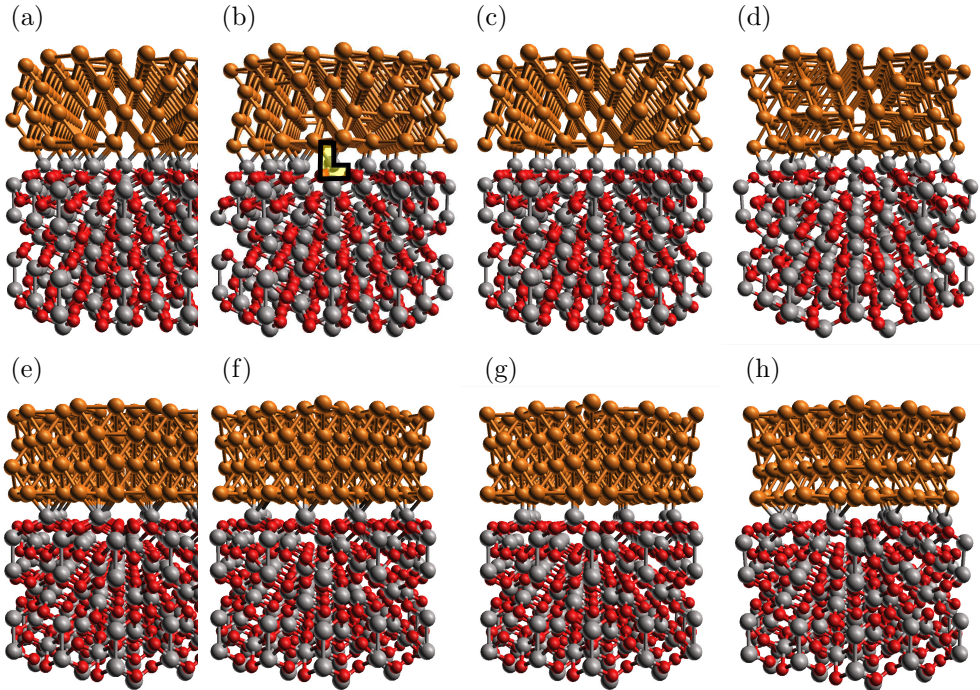FIG. 3. Cu/Al$_2$O$_3$ interface reconstructed.

FIG. 4. Cu/Al$_2$O$_3$ interface: a, e) the copper lattice stretched coherently to corundum spacings – initial configuration; b, f) after the input of first dislocation; c, g) the copper lattice stretched coherently to corundum spacings in the region of stacking fault; d, h) dislocation node formed by input of three partial dislocations. At the top, the crystallographic x-axis of corundum parallel to the paper; at the bottom, pointing out of the paper.

cells between the dislocations are formed. As was mentioned in the paper the distance between dislocations was about $14\,a_{\mathrm{Al_2O_3}}$. To reconstruct the periodic boundary conditions in preprocessed unit cell, it is assumed here that each nodal dislocation is associated with the next 5 dislocations situated on the left- and right-hand sides, cf. [8]. In result, the effect of 33 partial dislocations have been taken into account in the reconstruction (the sequence Aa, −Ab, Ac, −Ae, Ba, −Bc, Bg, Ca, −Ch, Cg, Ce, ...). This corresponds to the resultant displacements determined by solving iteratively the following implicit formula

$$\mathbf{u}(\mathbf{X}) = \sum_{j=1}^{n} \mathbf{f}_j\big(\mathbf{X} + \mathbf{u}(\mathbf{X})\big). \tag{25}$$

At the first step, the initial displacement of atoms was assumed to be

$$\mathbf{u}^0 = \sum_{j=1}^{n} \mathbf{u}_j(\mathbf{X}), \tag{26}$$

where $\mathbf{u}_j(\mathbf{X}) = \mathbf{f}_j\big(\mathbf{X} + \mathbf{u}_j(\mathbf{X})\big)$ was the resultant displacement obtained from the iteration process performed for a single j-th dislocation, cf. (17)–(20),

$$\Delta\mathbf{u}_j^{i+1}(\mathbf{X}) = -\big[\mathbf{1} - \boldsymbol{\beta}_j(\mathbf{X} + \mathbf{u}_j^i)\big]^{-1}\big[\mathbf{u}_j^i - \mathbf{f}_j(\mathbf{X} + \mathbf{u}_j^i)\big]. \tag{27}$$

The method has been used for reconstruction of the partial dislocation inserted by slips, see the stacking fault terminating the partial dislocations in Fig. 4b. Making the use of the method discussed above, a periodic cell of the interfacial zone of copper-corundum was reconstructed, see the green rhombus composing the base for a prism depicted in Fig. 2. For comparison, the junction corresponding to a stacking fault obtained by the rigid shift of copper on the Burgers vector $\frac{1}{6}\langle 112\rangle$ is shown in Figs. 4c and 4g.

In Fig. 4a, a fragment of the structure in the vicinity of a single dislocation node is shown. The structure has been generated by means of the Visual Editor of Crystal Defects [11], the atomic bonds have been generated by means of the Open Babel program [1].

In Fig. 3 only a fragment of the reconstructed interface with visible triangles of a coherent junction separated by triangles of stacking faults is shown. As a matter of fact, the introduction of three elemental stacking faults resulted in the formation of another ordering of copper atoms in relation to that initially assumed. Namely, at the beginning it was assumed that the copper atoms were situated on the top of oxygen atoms, see Figs. 4a and 4e. After introduction of partial dislocations the resultant junction in the all triangles of stacking faults corresponds to the location of interfacial copper atoms on top of aluminium atoms, see Figs. 4c and 4g.

The numerical solutions of the problem considered above were obtained in 4–5 iteration steps, with the accuracy identified with the norm of displacement vector change calculated for atoms in the given iteration step, $\frac{|\Delta\mathbf{u^{i+1}}|}{|\mathbf{u}^{i+1}|} < 10^{-6}$. In the previous papers, a detailed analysis of convergence tests for the method used here were carried out. For example, in [12], such an analysis was carried out for *single* dislocations in 4H-SiC.

6. Conclusions

In this paper, a nonlinear method for preprocessing the atomistic models of dislocations is discussed and tested. The key proposition of the new method was the observation that the analytical solutions obtained from the linear theory of dislocations hold the symmetry of lattice distortions in the spatial (real) configurations, while the reconstruction of atomistic models starts not from the deformed but from the perfect lattice. The iterative scheme for solving matrix equation sets implemented to preprocessing atomistic structures gives possibility for preparation of input data free of errors given by the previous method. On one hand, the iterative scheme starts from the analytical solutions available for dislocations, and on the other hand, the iterative scheme (16)–(20) limits as much as possible the inaccuracies of the direct use of the linear theory in preprocessing atomistic models of dislocations.

In the linear theory of dislocations, when writing $\boldsymbol{\varepsilon} = d\mathbf{u}/d\mathbf{x}$, it is not specified as to which configuration the differential form $d\mathbf{x}$ is related to. In practice, the elastic strains observed on the macro scale are usually so small that the difference between the Lagrangian and Eulerian configurations of the elastic body is negligibly small. Bearing in mind that the elastic limit in strain for the most engineering structures is below 0.1%, such an assumption often makes good sense. On the other hand, in the atomistic reconstructions of dislocations, the local lattice deformation is very large which resulted in the inaccuracies discussed in this paper.

From the viewpoint of the multiscale modelling, the nonlinear computational method presented in the paper can be used as a method for the preprocessing of input data for more accurate methods applied to the analysis of the physical and/or chemical properties of given variants of misfit dislocations arrangement. As a result, initial atomistic configurations near local energy minima are obtained, which enables the efficient reaching of the final non-random microstructures.

Acknowledgements

References

1. OpenBabel – The Open Source Chemistry Toolbox, software v. 2.2.3 available at http://openbabel.sourceforge.net.

2. P.M. Anderson, J.P. Hirth, J. Lothe, *Theory of Dislocations*, 3rd edition, Cambridge University Press, Cambridge, 2017.

3. I. Belabbas, G.P. Dimitrakopulos, J. Kioseoglou, J. Chen, J. Smalc-Koziorowska, First-principles investigation of *a*-line Shockley partial dislocations in wurtzite GaN: Core reconstruction and electronic structure, *Modelling and Simulation in Materials Science and Engineering*, **30**(8): 085004, 2022, https://doi.org/10.1088/1361-651X/ac9853.

4. A. Béré, A. Serra, Atomic structure of dislocation cores in GaN, *Physical Review B*, **65**: 205323, 2002, https://doi.org/10.1103/PhysRevB.65.205323.

5. A. Béré, A. Serra, On the atomic structures, mobility and interactions of extended defects in GaN: Dislocations, tilt and twin boundaries, *Philosophical Magazine*, **86**(15): 2159–2192, 2006, https:/doi.org/10.1080/14786430600640486.

6. B.A. Bilby, Continuous distribution of dislocations, [In:] I.N. Sneddon, R. Hill [Eds.], *Progress in Solid Mechanics*, Vol. 1, pp. 331–398, North-Holland, Amsterdam, 1960.

7. J.M. Burgers, *Proc. Acad. Sci. Amst.*, **42**: 293–378, 1939.

8. W. Cai, V.V. Bulatob, J. Chang, J. Li, S. Yip, Periodic image effects in dislocation modelling, *Philosophical Magazine*, **83**(5): 539–567, 2003, https://doi.org/10.1080/01418 61021000051109.

9. J. Chen, P. Ruterana, G. Nouet, Multiple atomic configurations of the a edge threading dislocation in GaN, *Computational Materials Science*, **82**(1-3): 117–119, 2002, https://doi.org/10.1016/S0921-5107(00)00754-6.

10. Y. Chen *et al.*, Interface intrinsic strengthening mechanism on the tensile properties of Al_2O_3/Al composites, *Computational Materials Science*, **169**: 109131, 2019, https://doi.org/10.1016/j.commatsci.2019.109131.

11. J. Cholewiński, P. Dłużewski, VECD – Visual Editor of Crystal Defects, 2012, software available at http://vecds.sourceforge.net.

12. J. Cholewiński, M. Maździarz, G. Jurczak, P. Dłużewski, Dislocation core reconstruction based on finite deformation approach and its application to 4H-SiC crystal, *International Journal for Multiscale Computational Engineering*, **12**: 411–421, 2014, https://doi.org/10.1615/IntJMultCompEng.2014010679.

13. R. deWit, Theory of disclinations: IV. Straight disclinations, *Journal of Research of the National Bureau of Standards—A. Physics and Chemistry*, **77A**(5): 607–658, 1973, https://doi.org/10.6028/jres.077A.036.

14. P. Dłużewski, G. Maciejewski, G. Jurczak, S. Kret, J.Y. Laval, Nonlinear FE analysis of residual stresses induced by misfit dislocations in epitaxial layers, *Computational Materials Science*, **29**(3): 379–395, 2004, https://doi.org/10.1016/j.commatsci.2003.10.012.

15. P. Dłużewski, T.D. Young, G. Dimitakopulos, Ph. Komninou, Continuum and atomistic modeling of the mixed straight dislocation, *International Journal for Multiscale Computational Engineering*, **8**(3): 331–342, 2010, https://doi.org/10.1615/IntJMultComp Eng.v8.i3.80.

16. S.V. Dmitriev, N. Yoshikawa, M. Kohyama, S. Tanaka, R. Yang, Y. Kagawa, Atomistic structure of the Cu(111)/α-Al$_2$O$_3$(0001) interface in terms of interatomic potentials fitted to ab initio results, *Acta Materialia*, **52**: 1959–1970, 2004, https://doi.org/10.1016/j.actamat.2003.12.037.

17. S.V. Dmitriev, N. Yoshikawa, M. Kohyama, R. Yang, S. Tanaka, Y. Kagawa, Modeling interatomic interactions across Cu/α–Al$_2$O$_3$ interface, *Computational Materials Science*, **36**: 281–291, 2006, https://doi.org/10.1016/j.commatsci.2005.03.015.

18. W. Dong *et al.*, A peridynamic approach to solving general discrete dislocation dynamics problems in plasticity and fracture: Part I. Model description and verification, *International Journal of Plasticity*, **157**: 103401, 2022, https://doi.org/10.1016/j.ijplas.2022.103401.

19. P. Dłużewski, J.Z. Domagala, S. Kret, D. Jarosz, M. Kryśko, H. Teisseyre, Phase-transition critical thickness of rocksalt Mg$_x$Zn$_{1-x}$O layers, *The Journal of Chemical Physics*, **154**(15): 154701, 2021, https://doi.org/10.1063/5.0042415.

20. F. Ernst, P. Pirouz, A.H. Heuer, HRTEM study of a Cu/Al$_2$O$_3$ interface, *Philosophical Magazine A*, **63**: 259–277, 1991.

21. J.P. Hirth, J. Lothe, *Theory of Dislocations*, Wiley, New York, 1982.

22. J. Kioseoglou, E. Kalesaki, L. Lymperakis, J. Neugebauer, Ph. Komninou, Th. Karakostas, Electronic structure of $1/6\langle20\overline{2}3\rangle$ partial dislocations in wurtzite GaN, *Journal of Applied Physics*, **109**: 083511, 2011, https://doi.org/10.1063/1.3569856.

23. K. Kondo, On geometrical and physical foundations of the theory of yielding, [In:] *Proceedings of the 2nd Japan National Congress for Applied Mechanics*, Tokyo, Vol. 2, pp. 41–47, 1952.

24. E. Kröner, Continuum theory of defects, [In:] R. Balian, M. Kleman, J.P. Poiries [Eds.], *Physics of Defects*, pp. 215–315, Nord-Holland, Amsterdam, 1981.

25. S. Liu *et al.*, Alignment of edge dislocations – the reason lying behind composition inhomogeneity induced low thermal conductivity, *Nature Communications*, **16**: 9775, 2025, https://doi.org/10.1038/s41467-025-64749-5.

26. Y. Long, N.X. Chen, Interface reconstruction and dislocation networks for a metal/alumina interface: An atomistic approach, *Journal of Physics: Condensed Matter*, **20**(13): 135005, 2008, https://doi.org/10.1088/0953-8984/20/13/135005.

27. A.E.H. Love, *Mathematical Theory of Elasticity*, Cambridge University Press, Cambridge, 1927.

28. L. Lymperakis, H. Abu-Farsakh, O. Marquardt, T. Hickel, J. Neugebauer, Theoretical modeling of growth processes, extended defects, and electronic properties of III-nitride semiconductor nanostructures, *Physica Status Solidi B*, **248**: 1837–1852, 2011, https://doi.org/10.1002/pssb.201046511.

29. T. Mizoguchi *et al.*, Chemical bonding, interface strength, and oxygen K electron-energy-loss near-edge structure of the Cu/Al_2O_3 interface, *Physical Review B*, **74**: 235408, 2006, https://doi.org/10.1103/PhysRevB.74.235408.

30. K. Nalepka, Efficient approach to metal/metal oxide interfaces within variable charge model, *The European Physical Journal B*, **85**: 45, 2012, https://doi.org/10.1140/epjb/e2011-10839-1.

31. K. Nalepka, Symmetry-based approach to parametrization of embedded-atom-method interatomic potentials, *Computational Materials Science*, **56**: 100–107, 2012, https://doi.org/10.1016/j.commatsci.2012.01.011.

32. K. Nalepka, Material symmetry: A key to specification of interatomic potentials, *Bulletin of the Polish Academy of Sciences. Technical Sciences*, **61**(2): 441–450, 2013, https://doi.org/10.2478/bpasts-2013-0043.

33. M.J.D. Powell, A new algorithm for unconstrained optimization, [In:] J.B. Rosen, O.L. Mangasarian, K. Ritter [Eds.], *Nonlinear Programming*, pp. 31–65, Academic Press, New York–London, 1970.

34. W.T. Read Jr., *Dislocations in Crystals*, McGraw-Hill, London, 1953.

35. C. Scheu *et al.*, Bonding at copper–alumina interfaces established by different surface treatments: A critical review, *Journal of Materials Science*, **41**: 5161–5168, 2006, https://doi.org/10.1007/s10853-006-0073-0.

36. S. Shi, S. Tanaka, M. Koyama, First-principles investigation of the atomic and electronic structures of α-$Al_2O_3(0001)/Ni(111)$ interfaces, *Journal of the American Ceramic Society*, **90**(8): 2429–2440, 2007, https://doi.org/10.1111/j.1551-2916.2007.01769.x.

37. C. Teodosiu, A dynamic theory of dislocations and its applications to the theory of the elastic plastic continuum, [In:] A. Simmonds *et al.* [Eds.], *Fundamental Aspects of Dislocation Theory*, Vol. 2, pp. 837–876, National Bureau of Standards Special Publication 317, US Government Printing Office, Washington, DC, 1970.

38. E.H. Yoffe, The angular dislocation, *Philosophical Magazine*, **5**: 161–175, 1960.

39. E.H. Yoffe, A dislocation at a free surface, *Philosophical Magazine*, **6**: 1147–1155, 1961.

40. T.D. Young, J. Kioseoglou, G.P. Dimitrakopulos, P. Dłużewski, P. Komninou, 3D modelling of misfit networks in the interface region of heterostructures, *Journal of Physics D: Applied Physics*, **40**(13): 4084, 2007, https://doi.org/10.1088/0022-3727/40/13/027.

41. W. Zhang, J.R. Smith, A.G. Evans, The connection between *ab initio* calculations and interface adhesion measurements on metal/oxide systems: Ni/Al_2O_3 and Cu/Al_2O_3, *Acta Materialia*, **50**: 3803–3816, 2002, https://doi.org/10.1016/S1359-6454(02)00177-5.

42. J. Łażewski *et al.*, DFT modelling of the edge dislocation in 4H-SiC, *Journal of Materials Science*, **54**(15): 10737–10745, 2019, https://doi.org/10.1007/s10853-019-03630-5.